Computers and Concrete, *Vol. 18, No. 1 (2016) 139-154*
DOI: http://dx.doi.org/10.12989/cac.2016.18.1.139

Post-cracking behavior of UHPC on the concrete members reinforced by steel rebar

H.A. Rahdar[a] and M. Ghalehnovi[*]

Civil Engineering Department, Faculty of Engineering, Ferdowsi University Of Mashhad, Mashhad, Iran

(Received November 22, 2015, Revised March 12, 2016, Accepted May 5, 2016)

Abstract. Since the concrete strength around the reinforcement rebar affects the tension stiffening, the tension stiffening effect of ultra high performance concrete on the concrete members reinforced by steel rebar is examined by testing the specimens with circular cross section with the length 850 mm reinforced by a steel rebar at the center of a specimen's cross section in this research. Conducting a tensile test on the specimens, the cracking behavior is evaluated and a curve with an exponential descending branch is obtained to explain the post-cracking zone. In addition, this paper proposes an equation for this branch and parameters of equation is obtained based on the ratio of cover thickness to rebar diameter (c/d) and reinforcement percentage (ρ).

Keywords: Ultra High Performance Concrete (UHPC); reinforcement; tension stiffening; reinforced concrete member; crack

1. Introduction

As a basic feature, tension stiffening focuses on the behavior of the reinforced concrete members under tension. Consider a reinforced concrete member which made by a reinforcement rebar surrounded by a concrete cylinder. The tension force exerts on the two ends of the rebar. Due to the bond between the concrete and rebar in their interface, the strains and stresses of the concrete cylinder increase with increasing force and crack occurs at a certain level of force where strains meet the cracking criterion. Creation of crack in the member results in the redistribution of internal strains and stresses in the member and the stiffness of the reinforced concrete member also changes. The increase of loading can produce more cracks in certain positions. For a reinforced concrete member, the process of loading increase occurs until the reinforcement rebar yields at one of two ends or the cracking cross section. Emergence of cracks in the concrete cylinder surrounding the reinforcement rebar affect on the stiffness and the behavior of the reinforced concrete member. This effect is called “tension stiffening” (Soltan Mohammadi 2010).

CEB-FIB (1993) and fib codes (1999a) propose similar stiffening models. In the model proposed by fib code (1999a), the force-strain relation of a concrete member reinforced by steel is

∗Corresponding author, Associate Professor, E-mail: ghalehnovi@um.ac.ir
[a]Ph.D. candidate, E-mail: rahdar@uoz.ac.ir

http://www.techno-press.org/?journal=cac&subpage=8 ISSN: 1598-8198 (Print), 1598-818X (Online)

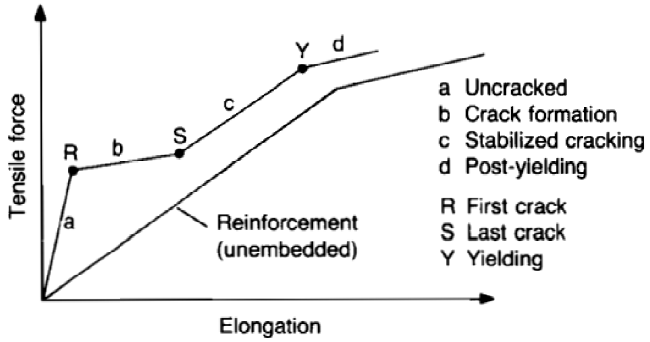

Fig. 1 Force-strain relation of a reinforced concrete member under tension (CEB-FIP 1993).

used (see Fig. 1).

In past, many researches are conducted on the tension stiffening effect of the concrete members reinforced by steel and the concrete with normal strength. their results show that tension stiffening of these members is considerable. Seong *et al*. (2011) presented a tension stiffening model. In reinforced concrete elements subjected to uniaxial tension, shear or flexure the proposed model enables the calculation of average tensile stresses in concrete, after yielding of reinforcement. The proposed model makes it possible to accurately calculate reinforcement stresses at crack locations and, thus, average strain conditions which result in rupture of reinforcement. This leads to more realistic predictions of the uniaxial, flexural, and shear ductility of reinforced concrete members. The tension stiffening effect of chemically pre stressed concrete (CPC) under uniaxial tension was experimentally investigated and compared with those of reinforced concrete (RC) by Raktipong Sahamitmongkol and Toshiharu Kishi (2010). The results of their study show that the CPC has superior tension stiffening than RC and the conventional model for RC substantially underestimates the tension stiffening of CPC. In addition, the number of cracks in CPC is less than in RC at the same load and the bond of CPC near loading and is higher than that of RC, although the average bond is almost same. Rim Nayal and Haydar A. Rasheed (2006) developed an inverse approach combining nonlinear numerical analysis and global experimental response to develop the tension stiffening model parameters needed to simulate homogenized concrete behavior in tension. The results of this study provided good model parameters to use in the case of concrete beams reinforced whit steel and fiber-reinforced polymer (FRP) bars. In a report, Elfgren and Noghabai (2002) used the results of seven groups of researchers on about 50 analyses and experiments on the tensile stiffness of the reinforcement rebars confined in reinforced concrete by considering parameters including the cover thickness, spacing between cracks, rebars size, tension stiffening of bare rebar and the softening effect of concrete. The studies of Ebead and Marzouk (2005) led to the presentation of a tension stiffening model for the concrete strengthened by FRP sheets to be used in the analysis of two-way slabs strengthened by FRP sheets. Stramandinoli and La Rovere (2008) presented a curve with an exponential descending branch to explain the post-cracking zone and in their Equation, the exponential decline parameter α is a function of the member yield ratio (ρ) and the ratio of steel to concrete modulus of elasticity (n). Testing the reinforced concrete specimens with the length 500 mm and the strength 26 MPa, Shayanfar *et al*. (2007) divided the resulting tensile strength curve, into four regions for the member and presented Equations for any region of the curve. Regarding the bond-slip and tension stiffening of the ordinary concrete with

FRP, Baena *et al*. (2013) presented a numerical model for analysis and compared its results with the experimental results. Yoo and Nemkumar Banthia (2015) simulated the flexural behavior of ultra-high-performance fiber-reinforced concrete (UHPFRC) beams reinforced with steel and glass fiber-reinforced polymer (GFRP) rebars. Chao-Wei Tang (2015) studied the local bond stress-slip behavior of reinforcing bars embedded in Lightweight aggregate concrete (LWAC).the result of this study show that the ultimate bond strength increased with the increase of concrete compressive strength. Calos Zanuy *et al*. (2009) presented the model to reproduce the distribution of longitudinal stresses and strains, bond stresses and relative slips along the crack spacing of a reinforced concrete tie with number of cycles. Deng Zong-cai *et al*. (2013) conducting the pull out test to investigate the bonding properties between high strength rebar and reactive powder concrete (RPC). The experimental results of the pullout and flexure tests conducted with HSS rebar in UHPC presented by saleem *et al*. (2013). Testing 35 direct tensile specimens, Lee and Kim (2009) examined the effect of the compressive strengths 20, 60 and 80 MPa on tension stiffening and crack response of the specimens. Yazici (2007) studied effect of condition curing and mineral additives with high-volume on the mechanical properties of the various compounds of ultra high performance concrete. Graybeal and Tanesi (2007) emphasized that the largest size of sand particles which used in construction UHPC is between 0.15 to 0.6 mm.

Since using ultra high performance concrete(UHPC) has attracted the attention of engineers due to its special features such as high compressive strength, low penetrability and resistance to frost cycles and also, because Less attention to the effect of tension stiffening for reinforced concrete members that UHPC are used to make them, In these research, doing a tensile test on the ultrahigh performance concrete specimens reinforced by steel rebars concrete, the tension stiffening effect is evaluated in the post-cracking stage by presenting an Equation.

2. Material properties, mixing process and preparation of specimens

2.1 Material properties

Ultra High Performance Concrete constituent materials are Portland cement, Silica fume, Quartz powder, Silica sand, superplasticizer and water.

The physical properties of the aggregates, used for this work, is descripted as follow:

• Quartz powder

Quartz powder is an important material in Ultra High Performance Concrete. Average diameter of its particles is 0.01 mm. Quartz powder is a hard material that improves the properties of the matrix.

• Silica sand

Sand particle size is limited to 0.8 mm, but not less than 0.15 mm. silica sand has advantages such as high hardness and easy access.

• Super Plasticizer

(Since water-cement ratio is very low for the Ultra High Performance Concrete, carboxylate-based Plasticizers is used to provide concrete slump.)

2.2 Mixing process

Firstly, the dry materials mix together until a homogeneous mixture achieve .This can take

Table 1 Characteristics of the specimens being tested

No.	Name of specimen	Diameter of specimen (mm)	Rebar diameter (mm)	Type of rebar	Cover	C/d*	ρ**
1	65-12-A2	65	12	A2	26.5	2.0	3.53
2	65-12-A3	65	12	A3	26.5	2.0	3.53
3	100-12-A2	100	12	A2	44.0	3.0	1.46
4	100-12-A3	100	12	A3	44.0	3.0	1.46
5	150-12-A2	150	12	A2	69.0	5.0	0.64
6	150-12-A3	150	12	A3	69.0	5.0	0.64
7	65-16-A2	65	16	A2	24.5	1.5	6.65
8	65-16-A3	65	16	A3	24.5	1.5	6.45
9	100-16-A2	100	16	A2	42.0	2.5	2.63
10	100-16-A3	100	16	A3	42.0	2.5	2.63
11	150-16-A2	150	16	A2	67.0	4.0	1.15
12	150-16-A3	150	16	A3	67.0	4.0	1.15

* c/d: Ratio of cover thickness to rebar diameter
** ρ: Reinforcement percentage

Table 2 the mix design of the concrete used to prepare the specimen

Materials	Content (kgf)
Cement	670.0
Silica fume	200.0
Quartz powder	285.0
Silica sand	1020.0
Superplasticizer (3%)	20.1
Water	178.0 (Liter)

Note: The values listed for a cubic meter of concrete.)

Table 3 Mechanical properties of ultra high performance concrete based on the results of the experiments

Mechanical properties	value
Compressive strength (MPa)	110.00
Modulus of elasticity (GPa)	41.18
Density (kgf/m^3)	2100.00
Splitting tensile strength of cylindrical concrete Specimens (MPa)	10.51
Direct Tensile strength (MPa)	9.00

several minutes. Then part of the water and half of the super plasticizer add to the mix. Mixing will continue until the materials completely combine. In the next step the remaining water and superplasticizer add to the mix.

Since in this research, ultra high performance concrete is used, the mix design and mechanical properties of the concrete are obtained from the related experiments and are given in Tables 2-3

2.3 Preparation of specimens

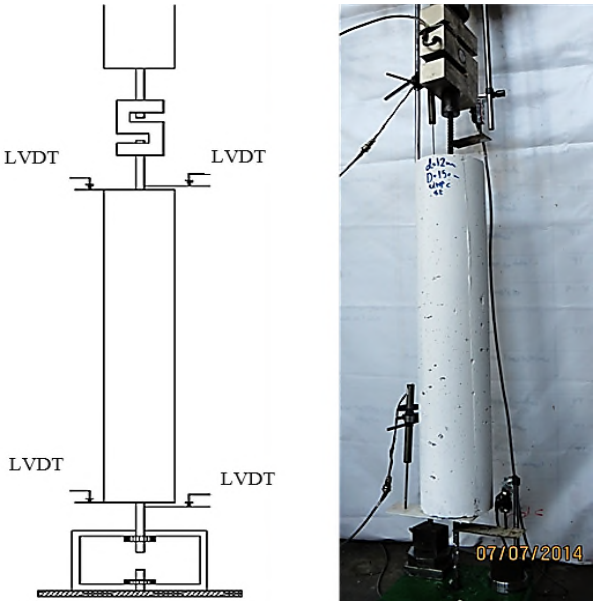

Fig. 2 Details and characteristics of the concrete specimens being tested

12 specimens of ultra high performance concrete with steel reinforcement were prepared and tested. Any test specimen has a circular cross section, at the center of which there is a steel rebar as a reinforcement. The length of specimens is 850 mm and the reinforcement rebar is exposed as 150 mm from both sides to be anchored in the tensile test device (Fig. 12). Two diameters of 12 and 16 mm are used to examine the effect of rebar diameter and the diameters 65, 100 and 150 mm for the specimens are chosen to apply the effect of concrete cover thickness (c/d) and reinforcement ratio (ρ) on the specimens. Two types of steel rebars A2 and A3 are also used to apply the effect of reinforcement properties such as modulus of elasticity and strength on the concrete member's tension stiffening.

Concrete specimens are generally denoted by X-Y-M. Where X denotes the diameter of the concrete specimen, Y denotes the diameter of the reinforcement rebar and M denotes the type of reinforcement rebar. For example, 100-12-A2 shows a concrete specimen with the diameter 100 mm reinforced by a steel rebar with the diameter 12 mm and the type of A2 at the center. The detailed characteristics of the specimens are given in Table 1.

For preparing the specimens, plastic cylindrical molds with the height 850 mm were first provided and the reinforcement rebar was placed at the center of the specimen's cross section using a suitable bench over which the molds were put, and the concrete was placed in the molds in three stages and for any stage, a vibrating table was used for proper compaction and removal of the concrete air.

3. Testing procedure

Specimens were preserved in vitro and after being processed for 28 days. tensile test was performed on them. In this test, the displacement speed of the tension jack is 0.7 mm/min. The

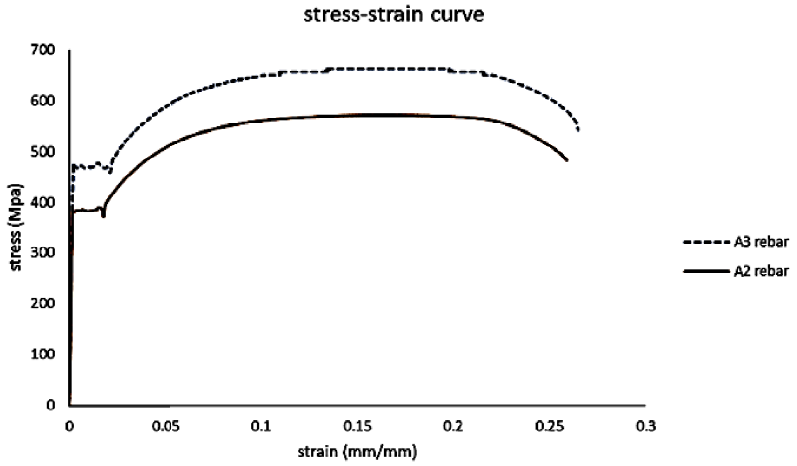

Fig. 3 Stress-strain curve of the rebars obtained from rebar tensile test

Table 4 Mechanical properties of rebars used based on the test results

Mechanical properties	Rebar type	
	A2	A3
Modulus of elasticity (GPa)	214.5	219.5
Yield strength (MPa)	399.18	478.00
Yield strain (mm/mm)	0.00233	0.00225
Ultimate strength (MPa)	571.00	663.00
Failure strain (mm/mm)	0.2584	0.2513

displacement of the rebar and that of concrete are recorded with a good precision by four LVDT. Those put above and below the specimen on the rebar and concrete. The force exerted on the specimen is also recorded by a load cell with the capacity 200 kN and the precision 0.01 kN at any moment. Data set is also prepared to be analyzed by a data card installed on a computer (see Fig. 2).

The specimens were photographed to record their behavior of cracks at different times to study the stages of crack propagation well

4. Test results

4.1 Stress-strain curve

4.1.1 Steel stress-strain curve

Tensile test was performed on several specimens of different rebars in order that the resulting stress-strain curve is used for comparison. This rebars used for making the specimens in the laboratory. Stress-strain curve and mechanical properties obtained for rebars in the test are presented in Fig. 3 and Table 4.

According to the stress-strain curves of the rebars A2 and A3 obtained in the test, the

mechanical properties of both types of rebars are calculated. The modulus of elasticity of the rebar A2 is 214.5 GPa and that of the rebar A3 is 219.5 GPa according to the curves (Fig. 3).

4.1.2 Stress-strain curves of the reinforced concrete specimens

Tensile test was performed on all reinforced concrete specimens. The purpose of the test was to determine the changes of the tensile strength of the reinforced concrete member in terms of the mean strain of rebar compared to the single rebar strength and to obtain the concrete's contribution to the tensile strength. Details of the test and notations of the specimens are presented in Fig. 2 and Table 1.

Curve of variations of total tensile strength of specimen (T/A_s) in terms of the mean strain (ε_{sm}) is shown in Figs. 4-5 (T: exerted force & A_s: rebar cross section). The curves show that the tensile

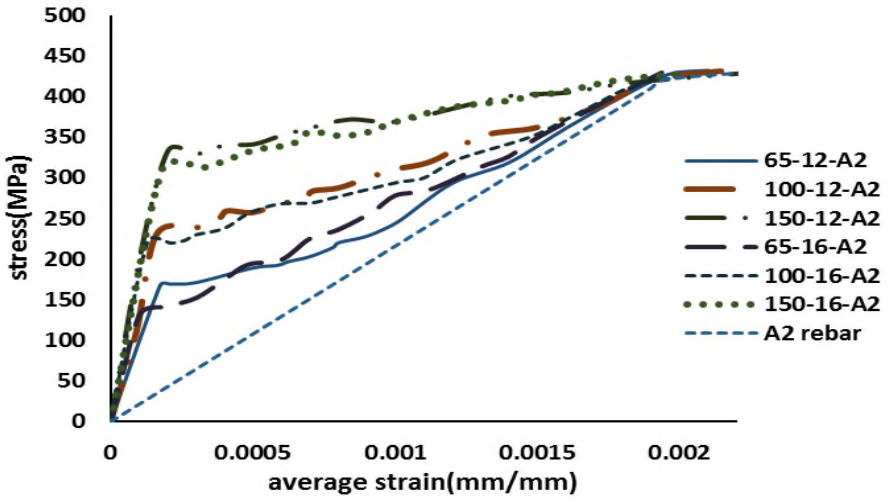

Fig. 4 Tensile strain-stress curve of ultra high performance concrete specimens reinforced by the rebar A2

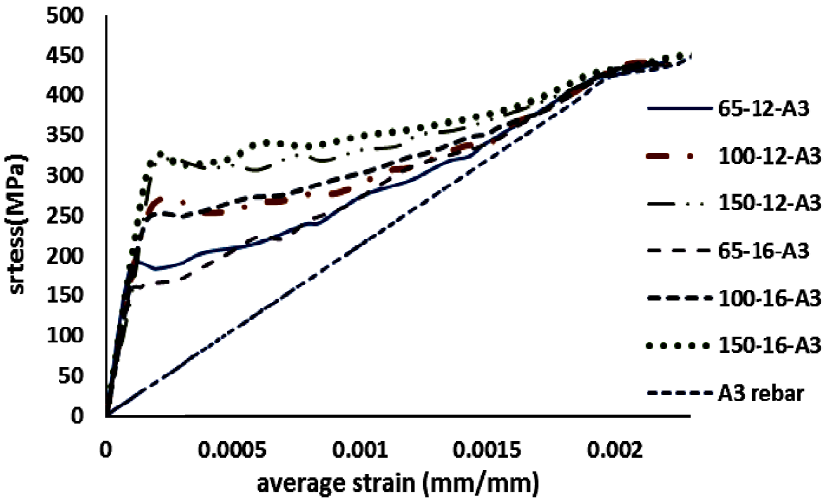

Fig. 5 Tensile strain-stress curve of ultra high performance concrete specimens reinforced by the rebar A3

strain-stress curve of a reinforced concrete member can be divided into three regions. The region (1) describes the member's elastic behavior from the beginning of loading to the beginning of the first crack. The region (2) shows the member's behavior from the first crack to the last crack. In this region, transverse cracks occur successively until the steady state is achieved. As it is also observed in the figures, the concrete's contribution significantly decreases after the first crack due to the occurrence of subsequent cracks to the final cracking point. The region (3) describes the member's behavior after the crack until the steel yields.

The comparison of the curves in Figs. 4-5 shows that the difference of the specimens' response is related to the steel content of the specimen's section and the rebar concrete cover thickness. For the specimens 150-16-A3, 150-16-A2, 150-12-A3 and 150-12-A2 whose steel content is low, the concrete's contribution to the specimen's total strength is significant compared the steel contribution. However, for specimens 65-16-A3, 65-16-A2, 65-12-A3 and 65-12-A2 whose steel content is high, the concrete's contribution to the tensile strength is negligible and steel has the highest contribution, so that the curve of the total strength changes of the reinforced concrete specimen is close to the single steel strength curve for these specimens.

Another point about Figs. 4-5 is that after the first crack occurred, the higher steel content makes later cracks occur more quickly and cracking reaches the crack stability point in lower mean strain. Also, specimens with a high steel content reach the yield point in a strain close to the bare steel yield strain, while specimens with a low steel content reach the yield point in a strain less than the bare steel yield strain due to the concrete's significant contribution and higher bond strength.

The comparison of the curves in Figs. 4-5 shows that for similar specimens, the change in rebar type from A2 to A3 has decreased the concrete's contribution to the specimen's total strength due to the higher strength and modulus of elasticity of the rebar A3.

4.1.3 tensile strain-stress curves of concrete's contribution

If the total tensile force exerted on the specimen is denoted by T, the following equilibrium Equation holds for any section

$$T = F_s + F_c \tag{1}$$

In the Equation above, F_s is the mean tensile force of the rebar's contribution that is obtained from the following Equation

$$F_S = A_S E_S \varepsilon_{sm} \tag{2}$$

ε_{sm} is the rebar's mean strain of the reinforced concrete specimen that is determined during the test for any exerted force T. A_s and E_s are the cross section and modulus of elasticity of the rebar, respectively.

The mean tensile force of the concrete's contribution is obtained from the Eq. (3).

$$F_C = T - F_S \tag{3}$$

The mean tensile stress of the concrete is determined by the following Equation for the reinforced concrete specimen

$$\sigma_C = F_C \big/ A_C \tag{4}$$

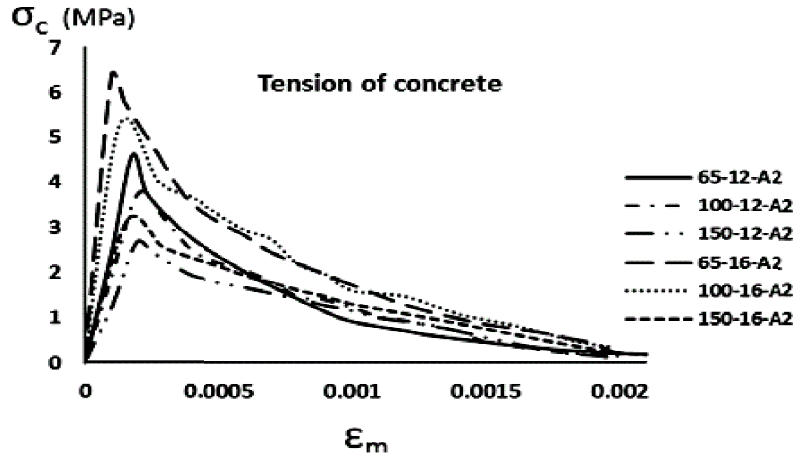

Fig. 6 The curve of the changes of the concrete's mean tensile stress versus the mean strain of the rebar A2

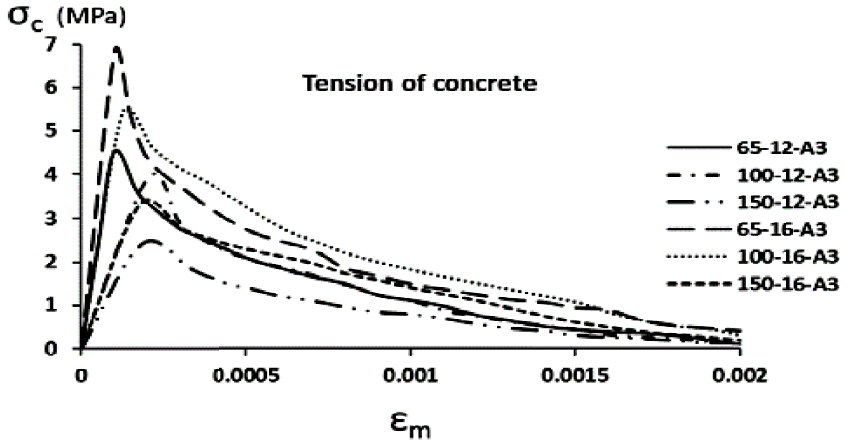

Fig. 7 The curve of the changes of the concrete's mean tensile stress versus the mean strain of the rebar A2

In the Equation above, A_c is the concrete's net cross section ($A_c=A_g-A_s$).

Using the Eq. (4), the changes of the concrete's mean tensile stress are obtained in terms of the rebar's mean strain. The application of the Equation is very important for nonlinear analysis of reinforced concrete structures by finite element method taking the smeared crack model into account. Using the Equation, a tension stiffening model can be obtained for the stress-strain curve of a reinforced concrete element that matches the actual behavior. The curve of the changes of effective tensile strength of the concrete's contribution (σ_c) versus rebar's mean strain (ε_{sm}) is presented in Figs. 6-7.

The curves show that the concrete's effective tensile strength has a linear elastic behavior before cracking. But after cracking, it has a descending branch that is call “concrete’s tension stiffening”. At first, the descending branch has a steep slope due to the quick occurrence of successive transverse cracks, but after reaching the steady state, it has a mild slope. Subsequently, the steel stress reaches the yield point in the cracks, but the specimen's mean strain and the steel

stress don’t reach the yield point in the spacing of two cracks that is due to uniform bond stresses in the spacing. Increasing the slip, there is no bond between the concrete and the steel and the effective tensile strength of the concrete approaches zero. The mean strain of the specimen will be also equal to the yield point strain of the rebar.

The strength of the curves obtained for specimens with different steel contents shows that at the beginning of the curve's descending branch, the effective tensile strength of the concrete's contribution for specimens with a low steel content is more than that of specimens with a high steel content. While after the stage of stability of crack, specimens with a low steel content have a lower tensile strength, because in this zone, the total tensile strength of reinforced concrete specimens is almost close to the bare steel strength and is similar for all specimens, and according to the inverse relation between stress and cross section and in similar force conditions, the tensile stress of the concrete's contribution is lower for specimens with a larger cross section (lower steel content).

5. Formulation of tensile behavior of ultra high performance concrete in reinforced concrete members with steel rebar

The curves in Figs. 6-7 show that the tensile behavior of ultra high performance concrete in reinforced concrete members under tension has two zones. The first zone is before cracking and the second zone is after cracking. For the reinforcement concrete specimens, before cracking in the reinforcement concrete, force divides between the concrete and reinforcement. Before cracking, Concrete contribution increases linearly until reaching the tensile strength of concrete (Eq. (5)). After cracking, by increasing the number of cracks in concrete, concrete contribution of stress tolerance gradually decreases exponentially. The ratio of the stress and strain of concrete after cracking to the cracking stress and strain is presented by Eq. (6).

Hence, the following Equations can be presented for tensile behavior of ultra high performance concrete in reinforced concrete members

Before cracking

$$\sigma_c = \left[\frac{\sigma_c^t}{\varepsilon_c^t}\right]\varepsilon_c \tag{5}$$

After cracking (descending branch)

$$\frac{\sigma_c}{\sigma_c^t} = \alpha \times e^{-\beta\left(\frac{\varepsilon_C}{\varepsilon_C^t}\right)} \tag{6}$$

In these Equations, $\sigma_c{}^t$ is the tensile stress of cracking and $\varepsilon_c{}^t$ is its equivalent strain.σ_c and ε_c are also the concrete's stress and strain, respectively. The parameters α and β are also obtained based on the results of experiments on the specimens for different reinforcement ratios (ρ) and thickness covers to diameter rebars ratios (c/d) that are shown in Figs. 8 to 11.

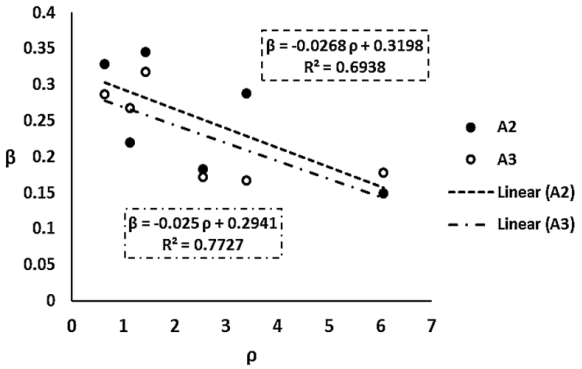

Fig. 8 The curve of the changes of β in terms of the reinforcement ratio (ρ)

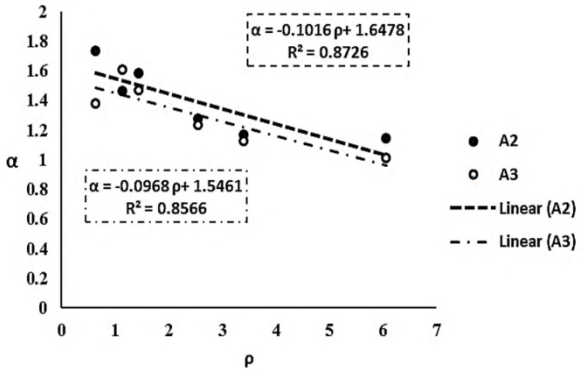

Fig. 9 The curve of the changes of α in terms of the reinforcement ratio (ρ)

Figs. 8- 9 show that increasing the reinforcement ratio (ρ), the parameters α and β decrease and for the rebar A3, their values are less than those for the rebar A2 that is due to the higher modulus of elasticity and strength of the rebar A3 compared to the rebar A2. For high reinforcement ratios, the effect of the change in the rebar type is lower on the parameter β.
According to the parameters α and β in the Eq. (6), the changes of these parameters in terms of ρ show that increasing the reinforcement ratio, the tension stiffening effect decreases.

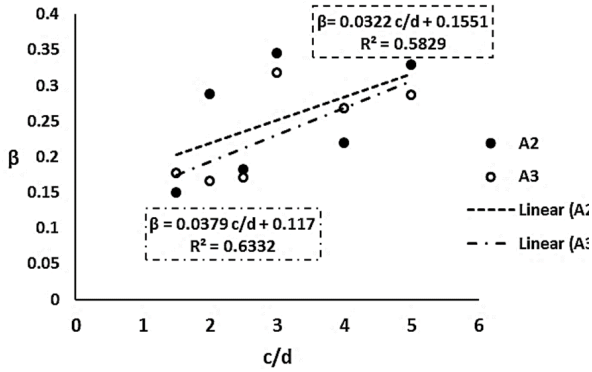

Fig. 10 the curve of the changes of β in terms of c/d

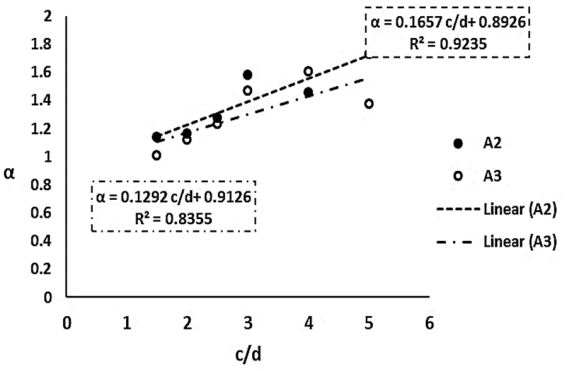

Fig. 11 the curve of the changes of α in terms of c/d

Figs. 10-11 show that increasing the reinforcement ratio (c/d), the parameters α and β increase and for the rebar A3, their values are less than those for the rebar A2 that is due to the higher modulus of elasticity and strength of the rebar A3 compared to the rebar A2. For high c/d ratios, the effect of the change in the rebar type is lower on the parameter β, while the effect is lower on parameter α for lower ratios.

6. Analysis of cracks

Fig. 12 The comparison of cracks of specimens with the rebar diameter 12 and the type A2 (forces in kgf)

In this section, the initial cracking force and the development range of cracks are presented for all specimens and finally, the spacing of cracks is compared for any specimen.

For the specimen 100-12-A2, the first crack occurred for the force 24.6 kN. Other cracks occurred for the forces 26, 27, 29, 30 and 37 kN in this specimen. The creation and development of cracks continued to the force range from 46 to 50 kN. The minimum and maximum spacing of cracks are 30 and 80 mm, respectively, and the mean spacing of cracks is 45 mm (see Fig. 12). The first crack occurred for the force 15 kN in the specimen 65-12-A2 and later cracks occurred for the forces 17, 19, 20, 23 and 26 kN and the cracks opened in the force range from 40 to 47 kN. The mean spacing of cracks is 50 mm in this specimen. For the specimen 150-12-A2, some cracks occurred suddenly for the force 39 kN. Subsequently, increasing the force to 48 kN, later cracks occurred. The creation and development stage of cracks continued to the force 52 kN in this specimen. In this specimen, the minimum and maximum spacing of cracks are 50 and 120 mm, respectively. The mean spacing of cracks is 68 mm for this specimen.

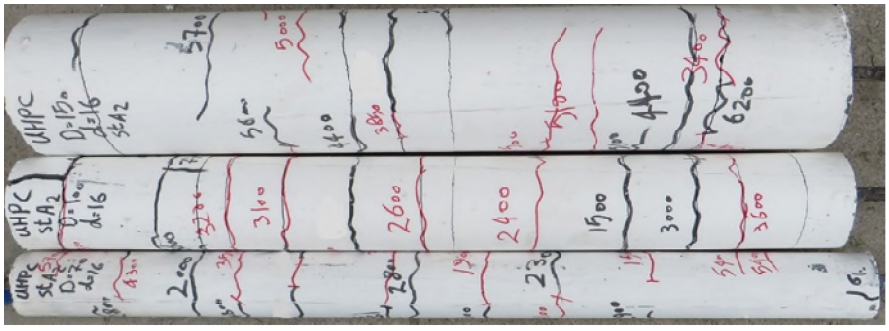

Fig. 13 The comparison of cracks of specimens with the rebar diameter 16 and the type A2 (forces in kgf)

According to Fig. 13, the first crack occurred for the force 34 kN for the specimen 150-16-A2. Other cracks occurred for the forces 44, 49, 51, 54 and 64 kN. The crack development and opening occurred for the force range from 70 to 78 kN and subsequently, crack was stable. The mean spacing of cracks is 58 mm, while minimum and maximum spacing of cracks are 36 and 80 mm, respectively. The distance between crack and edges of specimen is 80 mm. The first crack occurred for the force 19.5 kN in the specimen 65-16-A2 and later cracks occurred for the forces

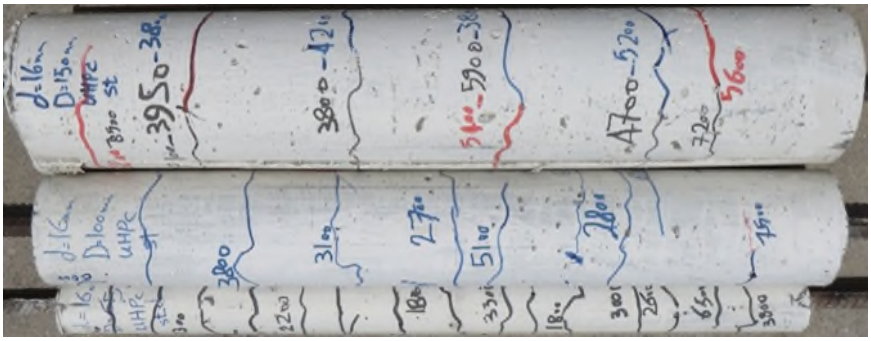

Fig. 14 The comparison of cracks of specimens with the rebar diameter 16 and the type A3 (forces in kgf)

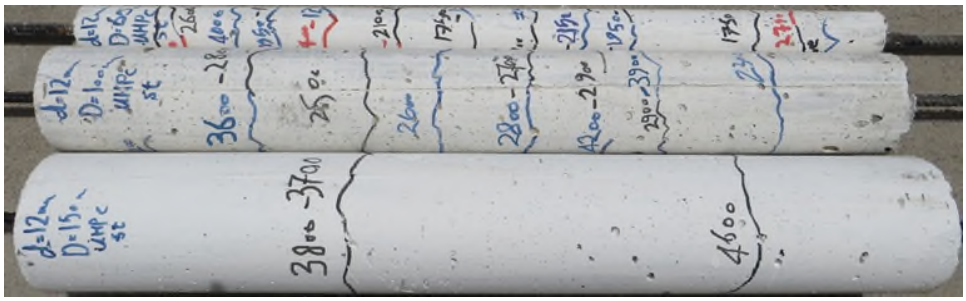

Fig. 15 The comparison of cracks of specimens with the rebar diameter 12 and the type A3 (forces in kgf)

23, 26, 28, 35 and 40 kN. The cracks developed in the force range from 43 to 51 kN and a small longitudinal crack occurred for the force 60 kN along the specimen. The mean spacing of cracks is 53 mm in this specimen, while the maximum spacing of cracks is 79 mm (Fig. 13).
Fig. 13 shows that the first crack occurred for the axial force 24.8 kN for the specimen 100-16-A2. Later cracks occurred for the forces 26, 31, 32 and 36 kN and one crack occurred for the force 70 kN. The cracks developed for the force range from 51 to 68 kN. The crack opening was well observed for the force 73 kN in this specimen. There was a longitudinal crack for the force 75 kN above the specimen between the second and third cracks (one third above the specimen) along the specimen. The minimum and maximum spacing of cracks are 60 and 85 mm, respectively, and the mean spacing of cracks is 72 mm in this specimen.

For the specimen 65-12-A3, the first crack occurred for the force 17 kN and the creation and development of cracks continued to the force 31 kN. The minimum and maximum spacing of cracks are 30 and 130 mm, respectively, and the mean spacing of cracks is 58 mm in this specimen. The initial cracking force is 26 kN in the specimen 100-12-A3 and later cracks developed up to the force 38 kN. The minimum and maximum spacing of cracks are 58 and 100 mm, respectively and the mean spacing of cracks is 74 mm in this specimen (Fig. 15). For the specimen 65-16-A3, the first crack occurred for the force 18 kN. The creation and development of cracks continued to the force 50 kN, and a longitudinal crack branched from the last transverse crack above the specimen for the force 53 kN. In this specimen, the minimum and maximum spacing of cracks are 40 and 80 mm, respectively, and the mean spacing of cracks is 60 mm (Fig. 14). Finally, the first crack occurred for the force 27 kN for the specimen 100-16-A3.The cracks developed up to the force 70 kN. The minimum and maximum spacing of cracks are 50 and 125

Table 5 The comparison of the initial cracking forces of the reinforced concrete member and the mean spacing of cracks

No.	Specimen	Initial cracking force (kN)	Mean spacing of cracks (mm)
1	65-12-A2	15.0	50
2	65-12-A3	17.0	58
3	100-12-A2	24.6	45
4	100-12-A3	26.0	74
5	150-12-A2	39.0	68
6	150-12-A3	39.5	185
7	65-16-A2	19.5	53
8	65-16-A3	18.0	60
9	100-16-A2	24.8	72
10	100-16-A3	27.0	79
11	150-16-A2	24.0	58
12	150-16-A3	38.0	103

mm, respectively, and the mean spacing of cracks is 79 mm in this specimen. To examine better, the results of the cracks analysis are presented in Table 5 that include the initial cracking force and the mean spacing of cracks.

The study of the crack behavior in the specimens being tested shows that increasing the concrete cover thickness on rebars, the initial cracking force increases in all specimens. In specimens with similar diameter, the increase in rebar diameter that leads to the increase in the reinforcement percent of the specimen increases its initial cracking force. On the other hand, the change in the rebar type has slightly affected the initial cracking force in specimens with similar diameter. Also, increasing the concrete cover thickness on rebars, the mean spacing of cracks has increased and the number of cracks has decreased. The increase in the reinforcement percent (increase of rebar diameter) for specimens with similar diameter resulted in the increase in the mean spacing of cracks. Although the modulus of elasticity of both types of rebar A2 and A3 is not largely different, the change in the rebar type in similar specimens has slightly increased the mean spacing of cracks.

7. Conclusions

In this research, the tension stiffening effect of ultra high performance concrete on the behavior of the concrete members reinforced by steel rebar was studied. The research was conducted by tensile test of 12 ultra high performance concrete specimens with circular cross section and the length 850 mm reinforced by a rebar at the center of specimen. The displacement speed of the tension jack was taken as 0.7 mm/min and the displacements and forces exerted on the specimen were recorded at any moment. According to the data obtained from experiments, the following results were obtained:

• According to the experimental results and curves related to the tension stiffening effect, it can be concluded that the presented experimental technique directly evaluates the tension stiffening

effect of ultra high performance concrete on the concrete members reinforced by steel rebar and is more suitable than other indirect procedures.

• Before the stage of crack formation, the initial stiffness ratio of specimens presents a good analysis of the tension stiffening effect. The ratio largely depends on the concrete specimen's reinforcement percent, and increasing the reinforcement ratio (ρ), the ratio decreases. Also for similar specimens, the ratio for the rebars A2 is more than the rebars A3, showing the increase in the concrete stiffening effect.

• For specimens with different steel contents at the beginning of the descending branch of the curve, the effective tensile strength of the concrete's contribution is more than the specimens with a high steel content for those with a low steel content. However, after the cracks were stable, specimens with a low steel content had a lower tensile strength, because in this zone, the tensile strength of reinforced concrete specimens is almost close to the bare steel strength and is similar for all specimens.

• Increasing the reinforcement ratio (ρ), the parameters α and β decrease and for the rebar A3, their values are less than those for the rebar A2 that is due to the higher modulus of elasticity and strength of the rebar A3 compared to the rebar A2. For high reinforcement ratios, the effect of the change in the rebar type is lower on the parameter β. According to the parameters α and β in the Equations presented, the changes of both parameters in terms of ρ show that the increasing the reinforcement ratio, the tension stiffening effect decreases.

• In crack stability stage, the mean spacing of cracks is less than the specimens of the rebar A3 for those of the rebar A2. Hence, the number of cracks is more than the specimens of the rebar A3 for those of the rebar A2 that results more decrease of the tension stiffening effect in these specimens.

As the increase of c/d ratio increased the initial stiffness, the force required for the beginning of the cracking stage has also increased.

References

Saleem, M.A., Mirmiran, A., Xia, J. and Mackie, K. (2012), "Development length of high-strength steel rebar in ultrahigh performance concrete", *J. Mater. Civil Eng.*, **25**(8), 991-998.

Baena, M., Torres, L., Turon, A. and Miàs, C. (2013), "Analysis of cracking behaviour and tension stiffening in FRP reinforced concrete tensile elements", *Compos. Part B: Eng.*, **45**(1), 1360-1367.

CEB-FIP (1993), *Model Code for Concrete Structures*, Committee Euro- International du Beton and Federation Internationale de la Precontrainte, Thomas Telford, London.

Zong-cai, D., Daud, J.R. and Chang-xing, Y. (2014), "Bonding between high strength rebar and reactive powder concrete", *Comput. Concrete*, **13**(3), 411-421.

Yoo, D.Y. and Banthia, N. (2015), "Numerical simulation on structural behavior of UHPFRC beams with steel and GFRP bars", *Comput. Concrete*, **16**(5), 759-774.

Ebead, U.A. and Marzouk, H. (2005), "Tension-stiffening model for FRP-strenghened RC concrete two-way slabs", *Mater. Struct.*, **38**(2), 193-200.

Elfgren, L. and Noghabai, K. (2002), "Tension of reinforced concrete prisms. Bond properties of reinforcement bars embedded in concrete tie elements. Summary of a RILEM round-robin investigation arranged by TC 147-FMB 'Fracture Mechanics to Anchorage and Bond'", *Mater. Struct.*, **35**(6), 318-325.

FIB (1999a), *Structural Concrete, Textbook on Behavior, Design and Performance*, Bulletin 1, federation internationale du beton, Lausanne, Switzerland, 224.

Graybeal, B. and Tanesi, J. (2007), "Durability of an ultrahigh-performance concrete", *J. Mater. Civil Eng.*, **19**(10), 848-854.

Lee, G.Y. and Kim, W. (2009), "Cracking and tension stiffening behavior of high-strength concrete tension members subjected to axial load", *Adv. Struct. Eng.*, **12**(2), 127-137.
Nayal, R. and Rasheed, H.A. (2006), "Tension stiffening model for concrete beams reinforced with steel and FRP bars", *J. Mater. Civil Eng.*, **18**(6), 831-841.
Sahamitmongkol, R. and Kishi, T. (2011), "Tension stiffening effect and bonding characteristics of chemically prestressed concrete under tension", *Mater. Struct.*, **44**(2), 455-474.
Lee, S.C., Cho, J.Y. and Vecchio, F.J. (2011), "Model for post-yield tension stiffening and rebar rupture in concrete members", *Eng. Struct.*, **33**(5), 1723-1733.
Shayanfar, M.A., Ghalehnovi, M. and Safiey, A. (2007), "Corrosion effects on tension stiffening behavior of reinforced concrete", *Comput. Concrete*, **4**(5), 403-424.
Soltan Mohammadi, M. (2010), "Stiffening behavior modeling elements reinforced with FRP reinforced concrete in pure tension", *J. Sharif Civil Eng.*, **26**(2), 11-19.
Stramandinoli, R.S. and La Rovere, H.L. (2008), "An efficient tension-stiffening model for nonlinear analysis of reinforced concrete members", *Eng. Struct.*, **30**(7), 2069-2080.
Tang, C.W. (2015), "Local bond stress-slip behavior of reinforcing bars embedded in lightweight aggregate concrete", *Comput. Concrete*, **16**(3), 449-466.
Yazici, H. (2007), "The effect of curing conditions on compressive strength of ultra high strength concrete with high volume mineral admixtures", *Build. Envir.*, **42**(5), 2083-2089.
Zanuy, C., Albajar, L. and de la Fuente, P. (2010), "On the cracking behaviour of the reinforced concrete tension chord under repeated loading", *Mater. Struct.*, **43**(5), 611-632.

CC

ACEM16/Structures16

The 2016 World Congress on

Civil, Environmental, & Materials Research and STRUCTURES

28 August – 1 September 2016 at ICC Jeju in Jeju Island, Korea

Congress Chair: **Chang-Koon Choi** (KAIST, Korea)

ACEM16 includes:

- □ Advances in Wind and Structures
- □ Geomechanics and Engineering
- □ Advances in Coupled Systems Mechanics
- □ Advances in Membrane Water Treatment
- □ Advances in Environmental Sci. & Tech.
- □ Advances in Materials Research

Strucutres16 includes:

- □ Advances in Concrete Construction
- □ Advances in Structural Monitoring & Maintenance
- □ Ocean Systems Engineering
- □ Advances in Computational Design
- □ Advances in Aircraft and Spacecraft Science

Mini Symposium organizers **are invited.**

Those interested in organizing a mini symposium at ACEM16/Structures16 should contact the Conference Secretariat for more information.

Organized by: **Korea Advanced Inst. of Science & Technology (KAIST)**
Int'l Association of Structural Eng. & Mechanics (IASEM)

In cooperation with: **Techno-Press** *International Journals*
http://www.techno-press.com

All correspondence should be addressed to:

Secretariat ACEM16/Structures16
P.O. Box 33 Yuseong, Daejeon 34186, Korea
E-mail: info@acem16.com, info@structures16.com
Website: http://acem16.com, http://structures16.com